Hindawi
Mathematical Problems in Engineering
Volume 2019, Article ID 5213759, 12 pages
https://doi.org/10.1155/2019/5213759

Research Article

A Hybrid Particle Swarm Optimization-Cuckoo Search Algorithm and Its Engineering Applications

Jinjin Ding,[1,2] **Qunjin Wang**,[3] **Qian Zhang**,[1,4] **Qiubo Ye**,[2] **and Yuan Ma**[3]

[1]*Department of Electrical Engineering and Automation, Anhui University, Hefei 230039, China*
[2]*Anhui Electric Power Research Institute, Hefei 230601, China*
[3]*Engineering Research Center of Power Quality, Ministry of Education, Anhui University, Hefei 230039, China*
[4]*National Engineering Laboratory of Energy-Saving Motor & Control Technology, Anhui University, Hefei 230039, China*

Correspondence should be addressed to Qian Zhang; qianzh@ahu.edu.cn

Received 8 November 2018; Revised 28 January 2019; Accepted 19 February 2019; Published 28 March 2019

Academic Editor: Oliver Schütze

This paper deals with the hybrid particle swarm optimization-Cuckoo Search (PSO-CS) algorithm which is capable of solving complicated nonlinear optimization problems. It combines the iterative scheme of the particle swarm optimization (PSO) algorithm and the searching strategy of the Cuckoo Search (CS) algorithm. Details of the PSO-CS algorithm are introduced; furthermore its effectiveness is validated by several mathematical test functions. It is shown that Lévy flight significantly influences the algorithm's convergence process. In the second part of this paper, the proposed PSO-CS algorithm is applied to two different engineering problems. The first application is nonlinear parameter identification for the motor drive servo system. As a result, a precise nonlinear Hammerstein model is obtained. The second one is reactive power optimization for power systems, where the total loss of the researched IEEE 14-bus system is minimized using PSO-CS approach. Simulation and experimental results demonstrate that the hybrid optimal algorithm is capable of handling nonlinear optimization problems with multiconstraints and local optimal with better performance than PSO and CS algorithms.

1. Introduction

Optimization problems are ubiquitous and critical in controller design [1], system identification [2], power systems [3], etc. These engineering problems are often nonlinear with various variables under complex constraints. Modern metaheuristic algorithms have been developed with an aim to carry out global search. The typical examples are Genetic Algorithm (GA) [4], PSO [5], etc. Two important characteristics of the metaheuristic algorithms are intensification and diversification. Intensification focuses around the current best solutions and selects the best candidates or solutions, while diversification makes sure that the algorithm can explore the search space more efficiently, often by randomization [6].

PSO and CS [6] are both relatively new evolutionary algorithms which can find optimal or suboptimal solutions in search space. PSO is a population-based heuristic global optimization technique. In this algorithm, the population is called a swarm, and the trajectory of each particle in the search space is dynamically adjusted by altering its velocity according to its own flying experience and swarm experience in the search space. CS is inspired by the interesting breeding pattern of cuckoos. In addition to the breeding behavior, cuckoos have been assumed to follow a Lévy flight movement pattern in the CS algorithm. The Lévy flight is a movement along a straight line followed by sudden turns in random directions. The attributes of the CS allow enhanced exploration of the search space in comparison with other evolutionary computing algorithms. Since the PSO and CS algorithms are both inspired by the survival and migration of avifauna, it is nature to utilize the superiority of Cuckoo Search algorithm with the purpose of improving the searching ability of traditional particle swarm optimization algorithm [7].

Some studies are undertaken in the improvement of traditional metaheuristic algorithms [8–10]. In [8], the MapReduce programming paradigm is implemented in

the Apache Spark tool. The Cuckoo Search binary algorithm is proposed and applied to different instances of the crew scheduling problem. In [9], the modifications of the original CS algorithms are summarized. The continuous, binary, and multiobjective CS algorithms are compared both in the aspects of benchmark tests and in the applications.

In our former work, the advanced PSO algorithm was applied to nonlinear parameters identification of motor drive servo system [10, 11]. In [10], a switched nonlinear model is proposed to the description of multistates in motor servo system, and former algorithm is able to deal with the nonlinear multiobjective problem with constraints. Our recent researches show that the success rate can be further increased with less iteration times among the convergence process by the combination of PSO and CS.

This paper aims to formulate a new algorithm named Particle Swarm Optimization-Cuckoo Search (PSO-CS) and analyzes its performance through numerical computing and industrial applications. The major contributions of this paper are (i) the improvement of success rate and convergence iteration for the hybrid PSO algorithm and (ii) the improved method is applied to two totally different application; both results are better than traditional algorithm.

The first application deals with the nonlinear parameter identification of a motor drive radar antenna servo system. A Hammerstein structure nonlinear model is introduced to describe the nonlinear elements, such as friction, dead-zone, and backlash of the servo system. The PSO-CS algorithm plays a critical part in the Hammerstein model parameter estimation. The comparison of field data and model output demonstrates the effectiveness of the algorithm and validates the optimal results. In the second application, the optimal reactive power dispatch problem (ORPD) for standard IEEE systems is realized by the CS-PSO algorithm. The fitness function of the optimization model is the total loss of the power system. The nodal voltages of generators, reactive power compensations, and transformer taps are optimized in the IEEE 14-bus system. The simulation result proves the feasibility and improved searching ability of the proposed algorithm.

2. Overview of PSO and CS

2.1. Particle Swarm Optimization Background. The swarm $\{X_i,\ i = 1, \ldots, N\}$, which has N particles is considered in the standard PSO. In D-dimensional space, the i_{th} particle $X_i = \{x_{i1}, \ldots, x_{iD}\}$ is a potential solution to the researched problem. The velocity of the i_{th} particle is $V_i = \{v_{i1}, \ldots, v_{iD}\}$. For the i_{th} particle, the best position in the t_{th} step is expressed as $Pbest_i(t) = \{Pbest_{i1}(t), \ldots, Pbest_{iD}(t)\}$.

Meanwhile, the best position of the entire swarm is defined as $Gbest(t) = \{Gbest_1(t), \ldots, Gbest_D(t)\}$. Thus at the $(t+1)_{th}$ step, the new position of the i_{th} particle is calculated as below.

$$x_{ij}(t+1) = x_{ij}(t) + v_{ij}(t+1) \tag{1}$$

$$\begin{aligned} v_{ij}(t+1) = {} & w \times v_{ij}(t) + c_1 \times rand1 \\ & \times \left[Pbest_{ij}(t) - x_{ij}(t)\right] + c_2 \times rand2 \\ & \times \left[Gbest_j(t) - x_{ij}(t)\right] \end{aligned} \tag{2}$$

where $x_{ij}(t)$ and $v_{ij}(t)$ represent the position and velocity of the i_{th} particle with respect to the j_{th} dimension, w is the inertia weight factor, c_1 and c_2 are two positive constants called acceleration coefficients, and *rand1* and *rand2* are two uniformly distributed random values in the range [0, 1].

2.2. Cuckoo Search and Lévy Flights

2.2.1. Key Step of Cuckoo Search. CS is a kind of nature-inspired metaheuristic algorithms, and the aggressive reproduction strategy of special cuckoo species stimulates the proposal of CS. Three idealized rules [6] are delimited, and the last rule means introducing some new random solutions in the algorithm. It can be approximated by a friction p_a of the n host nests to produce new nests.

Following the cuckoo breeding behavior which can be found in [12] and was summarized in [13], and the basic steps of the CS can be determined. The optimization problem to be solved is described as an objective function $f(X)$, $X = \{x_1, \ldots, x_D\}$ in the D-dimensional space. In order to elaborate the constructional details of the PSO-CS algorithm, we normalized the variables of CS with PSO.

There are N host nests $\{X_i,\ i = 1, \ldots, N\}$ within the specified search space. Each nest $X_i = \{x_{i1}, \ldots, x_{iD}\}$ (the representations are the same with the particle X_i in PSO) represents a possible solution of the optimization problem to be solved. One of the key steps of the CS is searching for the new population of nests $X_i(t+1)$. Furthermore, the new nests are obtained using Lévy flight as follows:

$$x_{ij}(t+1) = x_{ij}(t) + \alpha \oplus Lévy(\lambda) \tag{3}$$

where α is the step size, $\oplus$ represents the entry-wise multiplication operation, and λ is a Lévy flight parameter.

2.2.2. Lévy Flights. Lévy flight is a kind of random walk with the step length which has the Lévy distribution. It is introduced to the CS algorithm to get a Lévy-flight-style intermittent scale-free search pattern. In [9], it is demonstrated that Lévy flights are able to maximize the efficiency of resource searches in the uncertain environment. The Lévy distribution is defined as

$$L(s, \gamma, \mu) = \begin{cases} \sqrt{\dfrac{\gamma}{2\pi}} \exp\left[-\dfrac{\gamma}{2(s-\mu)}\right] \dfrac{1}{(s-\mu)^{3/2}} & 0 < \mu < s < 0 \\ 0 & otherwise \end{cases} \tag{4}$$

where $\mu > 0$ is a minimum step and γ is a scale parameter. In Mantegna's algorithm, the step length s can be calculated by

$$s = \frac{u}{|v|^{1/\beta}} \tag{5}$$

where u and v are drawn from normal distribution. That is,

$$u \sim N\left(0, \sigma_u^2\right), \quad v \sim N\left(0, \sigma_v^2\right) \tag{6}$$

$$\sigma_u = \left\{ \frac{\Gamma(1+\beta)\sin(\pi\beta/2)}{\Gamma\left[(1+\beta)/2\right]\beta 2^{(1+\beta)/2}} \right\}^{1/\beta}, \quad \sigma_v = 1 \tag{7}$$

where $\Gamma(z)$ is the Gamma function $\Gamma(z) = \int_0^\infty t^{z-1}e^{-t}dt$. In the case when $z = n$ is an integer, $\Gamma(n) = (n-1)!$

3. Particle Swarm Optimization-Cuckoo Search Algorithm with Lévy Flights

It is mentioned that the entry-wise product $\oplus$ is similar to that used in PSO, but the random walk via Lévy flight is more efficient in exploring the search space as its step length is much longer in the long run. Because a power-law distribution is often linked to some scale-free characteristics, the Lévy flight can thus show self-similarity and fractal behavior in flight patterns [14]. Naturally, with the purpose of improving the performance of PSO, the Lévy flight is considered to replace the random searching method of traditional PSO algorithm. Therefore, the modified PSO algorithm is named PSO-CS.

3.1. PSO – CS Algorithm. The searching ability of PSO is influence by random variables *rand1* and *rand2*, when we set the parameters w, c_1, and c_2 as fixed values [15]. We introduced the Lévy flight for the change of random step length. Thus the formed PSO-CS algorithm is detailed as follows.

Step 1. The priori values of parameters are initialized, such as population size of swarm (N), minimum and maximum weights ($W_{\min}, W_{\max}$), and acceleration coefficients (c_1, c_2).

Step 2. The lower and upper bounds for each particle and the particles' velocities are specified in different neighborhood.

Step 3. The first generation of particles is randomly initialized within the specified space, $X_i = \{x_{i1}, \cdots, x_{iD}\}$, $i = 1$,

while $t <$ *MaxGeneration* or other stop criterion.

Step 4. The fitness function of each particle $f(X_i) = f_i$ is evaluated. The best position $Pbest_i(t)$ and the best position of the whole swarm $Gbest(t)$ are found (similar to PSO).

$$Pbest_i(t+1) = \begin{cases} x_i(t+1) & \text{if } f\left(x_i(t+1)\right) < f\left(x_i(t)\right) \\ Pbest_i & otherwise, \end{cases} \tag{8}$$

$$Gbest(t) = \min\left\{Pbest_1(t), Pbest_2(t), \ldots Pbest_N(t)\right\}$$

Step 5. A friction p_a of the worst performing particle is chosen in terms of the fitness function. The selected particles should be abandoned, and then the replacement of randomly generated ones is undertaken within the specified search space (similar to CS).

Step 6. The inertia weight w is updated as

$$w = W_{\max} - \frac{W_{\max} - W_{\min}}{T} \times t \tag{9}$$

The velocity V_i and position X_i of each particle are updated according to Formulas (1) and (2). Parameters *rand*1 and *rand*2 vary with Lévy flight pattern following (4) to (7), which is different from the former PSO (hybrid of PSO and CS).

$$\begin{aligned} v_{ij}(t+1) = {} & w \times v_{ij}(t) + \left(c_1 \oplus Lévy(\lambda)\right) \\ & \times \left[Pbest_{ij}(t) - x_{ij}(t)\right] \\ & + \left(c_2 \oplus Lévy(\lambda)\right) \\ & \times \left[Gbest_j(t) - x_{ij}(t)\right], \\ x_{ij}(t+1) = {} & x_{ij}(t) + v_{ij}(t+1) \end{aligned} \tag{10}$$

Step 7. The iteration step increases ($t = t+1$). The termination criterion is always the terminating generation or the ultimate value of fitness function, as other metaheuristic algorithms. If the termination criterion is not met, go to Step 4. Else return X_{best} as the final solution to the optimization problem.

End while

Step 8. List the optimization results. Meanwhile plot each value of the best fitness function in the optimization processing.

The population size of swarm N depends on the dimension of the problem. The parameters in the hybrid algorithm are problem-dependent [15] as the traditional PSO and CS algorithms. They are often determined after analysis and optimized by repeated calculation. For the performance analysis and parameter selection of the proposed method, a Monte Carlo method which is used in the research of traditional particle swarm optimization [16] can be introduced to obtain a set for fixed parameters. Besides, $\Gamma(z) = \int_0^\infty t^{z-1}e^{-t}dt$ is realized by Gamma function $\Gamma = gamma(z)$ using MATLAB.

The inertia weight changes from $W_{\min}$ to $W_{\max}$. The friction p_a controls the launching of a random long-distance exploration strategy, reflecting the probability whether the nest will be abandoned or be updated [17]. The higher the value of this parameter, the closer the search process is to the random search.

3.2. Benchmark Function Test. Eight benchmark functions [17] are chosen to evaluate the performance of the hybrid PSO-CS algorithm with the sizes of functions varying from 10 to 100. Definitions of benchmark problems are described as follows:

(1) Sphere function

$$f_1(x) = \sum_{i=1}^{d} z_i^2, \quad z = X - O, \ o = [o_1, o_2, \ldots, o_D]; \tag{11}$$

(2) Rosenbrock function

$$f_2(x) = \sum_{i=1}^{d-1} \left[100\left(x_i^2 - x_{i+1}^2\right)^2 + \left(x_i - 1\right)^2 \right]; \tag{12}$$

(3) Shifted Schwefel's function

$$f_3(x) = \sum_{i=1}^{d} \left[-z_i \sin\left(\sqrt{|z_i|} \right) \right], \quad z = X - O, \ o = [o_1, o_2, \ldots, o_D]; \tag{13}$$

(4) Shifted Ackley's function

$$f_4(x) = -20 \exp\left[-0.2 \sqrt{\frac{1}{d} \sum_{i=1}^{d} z_i^2} \right] - \exp\left[\frac{1}{d} \sum_{i=1}^{d} \cos\left(2\pi z_i\right) \right] + (20 + e), \quad z = X - O, \ o = [o_1, o_2, \ldots, o_D]; \tag{14}$$

(5) Shifted Griewank's Function

$$f_5(x) = \frac{1}{400} \sum_{i=1}^{d} z_i^2 - \prod_{i=1}^{d} \cos\left(\frac{z_i}{\sqrt{i}} \right) + 1, \quad z = X - O, \ o = [o_1, o_2, \ldots, o_D]; \tag{15}$$

(6) Shifted rotated Griewank's Function

$$f_6(x) = \frac{1}{400} \sum_{i=1}^{d} z_i^2 - \prod_{i=1}^{d} \cos\left(\frac{z_i}{\sqrt{i}} \right) + 1, \quad z = M(X - O), \ cond(M) = 3, \ o = [o_1, o_2, \ldots, o_D]; \tag{16}$$

(7) Shifted Rastrigin's function

$$f_7(x) = \sum_{i=1}^{d} \left[z_i^2 - 10\cos\left(2\pi z_i\right) + 10 \right], \quad z = X - O, \ o = [o_1, o_2, \ldots, o_D]; \tag{17}$$

(8) Shifted rotated Rastrigin's function

$$f_7(x) = \sum_{i=1}^{d} \left[z_i^2 - 10\cos\left(2\pi z_i\right) + 10 \right], \quad z = M(X - O), \ cond(M) = 2, \ o = [o_1, o_2, \ldots, o_D]. \tag{18}$$

Some indexes are introduced for the comparison of different algorithms. MFV and SDFV stand for the mean and the standard deviation of the function value. Sometimes the convergence process falls into the local optimum failing to find the global optimal solution. The success rate is introduced as the percentage of reaching the global solution within specified error range. Confidence C represents the success rate by counting the number of optimization runs with an objective function value within a precision of $1E-4$ from the optimum function value for all 200 runs. The details of benchmark test functions are listed in Table 1.

Table 1: Benchmark functions.

Test functions	Search space	Global optimum x^*	d
f1	$[-5.12, 5.12]$	o	4
f2	$[-2.4, 2.4]$	$(1, 1, 1, 1, 1)$	5
f3	$[-500, 500]$	$(420.9687, 420.9687)$	2
f4	$[-32.768, 32.768]$	o	2
f5	R	o	3
f6	R	o	3
f7	$[-5, 5]$	o	2
f8	$[-5, 5]$	o	2

Table 2: Parameter study of p_a in Ackley's function test.

p_a	time	MFV
0.05	1.177	9.3914e-06
0.1	0.7684	6.6760e-06
0.15	0.5439	6.3443e-06
0.2	0.5116	2.9924e-06
0.25	0.4539	3.5629e-07
0.3	0.4739	2.4210e-06
0.4	0.5055	4.0667e-06
0.5	0.66015	8.5684e-06

In the numerical experiment, the numbers of host nests n and the friction p_a are selected as trial variables. Usually, $N = 15$ to 50 are sufficient for most optimization problems. As parameter p_a is a new parameter for the proposed PSO algorithm, the parameter study is undertaken in Ackley's function test in 10D. The results are shown in Table 2. It is demonstrated that the proposed algorithm has good performance in convergence time and accuracy when $p_a = 0.15$ to 0.30. This conclusion is similar to the research by Yang [13].

Therefore, after a large number of experimental programming and the parameter adjustment, the fixed parameters $N = 20$, $c_1 = c_2 = 1$, $W_{\max} = 0.9$, $W_{\min} = 0.4$, $p_a = 0.25$, and $\beta = 3/2$ are used in the simulations. The results are shown in Tables 3–6.

The algorithm is coded in MATLAB 2017a, and experiments are made on i7-5600U CPU with a Pentium 2.6 GHz Processor and 8.00 GB of memory. The above benchmark functions f1 to f8 are tested in 10-dimension (10D), 30-dimension (30D), 50-dimension (50D), and 100-dimension (100D). For all test functions, the algorithms carry out 200 independent runs. The eight benchmark functions are tested in 10D and compared with PSO, CS and GA-PSO as shown in Table 3.

Table 3: Comparison of PSO-CS algorithm with the original PSO and CS algorithms on 10D problem.

Functions	Indexes	PSO-CS	PSO	CS	GA-PSO [5]
Function F1 Dim=10	*MFV*	4.81e-04	9.069e-03	7.752e-03	5.673e-03
	SDFV	5.125e-07	4.796e-06	3.613e-06	1.721e-06
	C	100%	100%	100%	100%
Function F2	*MFV*	2.495e+01	8.031e+02	7.972e+02	3.546e+02
Dim=10	*SDFV*	3.510e+02	6.39e+02	3.986e+02	4.620e+02
	C	100%	91%	91%	98%
Function F3	*MFV*	-4.192e+03	-5.735e+03	-4.013e+04	-5.301e+04
Dim=10	*SDFV*	7.64e+01	9.127e+02	2.048e+02	1.846e+02
	C	100%	92%	95%	99%
Function F4	*MFV*	0.000e+00	1.677e-03	2.23e-03	1.342e-04
Dim=10	*SDFV*	4.419e-10	0.000e+00	0.000e+00	0.001e+03
	C	100%	90%	97%	97%
Function F5	*MFV*	6.3582e+04	8.1716e+03	7.5484e+03	9.100e+04
Dim=10	*SDFV*	7.500e+03	2.249e+02	2.943e+02	8.301e+03
	C	100%	100%	100%	100%
Function F6	*MFV*	2.8735e+01	4.4293e+01	1.1336e+01	9.3499e+02
Dim=10	*SDFV*	1.348e+01	1.676 e+01	2.892 e+02	2.201e+02
	C	100%	95%	98%	98%
Function F7	*MFV*	1.6745e+01	6.4205e+00	2.3136e+01	5.1514e+01
Dim=10	*SDFV*	2.956e+01	1.9657e+00	4.061e+01	9.6007e+01
	C	100%	99%	99%	99%
Function F8	*MFV*	1.7391e+00	1.4661e+01	1.5014 e+01	3.0457e+00
Dim=10	*SDFV*	2.934e+00	8.0252e+00	7.212 e+00	3.237e+00
	C	99%	93%	94%	94%

Table 4: Comparison of PSO-CS algorithm with the original PSO and CS algorithms on 30D problem.

Functions	Indexes	PSO-CS	PSO	CS	GA-PSO [5]
Function F1 Dim=30	*MFV*	4.727e-04	6.32e-04	5.73e-04	5.021e-04
	SDFV	6.218e-06	7.61e-07	1.38e-07	1.56e-07
	C	99%	98%	99%	99%
Function F2	*MFV*	3.471e+01	1.34e+03	9.23e+02	7.023e+02
Dim=30	*SDFV*	8.15e+02	2.11e+03	1.7216e+03	3.347e+02
	C	100%	90%	90%	92%
Function F3	*MFV*	-1.256e+04	-1.146e+04	-1.255+04	-1.162e+04
Dim=30	*SDFV*	2.75e+02	5.82e+02	5.26e+02	3.566e+02
	C	98%	90%	91%	95%
Function F4	*MFV*	3.273e-06	1.9e-01	1.8e-01	1.539e-02
Dim=30	*SDFV*	3.001e-07	1.00e-03	2.1e-02	8.02e-04
	C	99%	89%	95%	96%

For the 30D, 50D, and 100D problems, we also conduct four different experiments for comparison with different groups of algorithms the same as those for the 10D problems. The detailed results are summarized in Tables 4–6.

The comparison results in Tables 3–5 can be summarized as follows. For the test functions in all the 10/30/50/100 dimensions, the proposed PSO-CS can find better optimal or close-to-optimal solutions with smaller standard deviations than traditional PSO, CS, and GA-PSO. These results also indicate the Lévy flights and worst solution abandon can effectively improve the performance of the hybrid algorithm, especially for 30 or lower dimensional problems. Note that the number of individuals N should not be too large. Otherwise, the optimal results may not be available.

It is possible that the standard PSO fails to find the global optimum in the Rosenbrock and Ackley problems [10]. The

Table 5: Comparison of PSO-CS algorithm with the original PSO and CS algorithms on 50D problem.

Functions	Indexes	PSO-CS	PSO	CS	GA-PSO [5]
Function F1	*MFV*	3.191e-01	8.231e+01	3.09e+01	2.845e+01
Dim=30	*SDFV*	2.94e-02	1.348e+02	5.7e+02	3.689e+02
Dim=50	*C*	82%	71%	70%	70%
Function F2	*MFV*	9.855e+01	6.073e+03	5.903e+03	3.834e+03
Dim=50	*SDFV*	6.725e+02	1.678e+04	8.325e+03	9.560e+02
	C	84%	70%	70%	76%
Function F3	*MFV*	-2.094e+04	-2.073e+04	-2.092e+04	-2.8373+04
Dim=50	*SDFV*	6.477e-04	4.381e-02	6.557e-04	7.638e-04
	C	85%	73%	81%	85%
Function F4	*MFV*	5.141e-04	3.874e-03	8.783e-04	6.273e-04
Dim=50	*SDFV*	6.453e-06	9.425e-04	3.214e-06	4.385e-05
	C	79%	60%	67%	70%

Table 6: Comparison of PSO-CS algorithm with the original PSO and CS algorithms on 100D problem.

Functions	Indexes	PSO-CS	PSO	CS	GA-PSO [5]
Function F1	*MFV*	1.231e+00	3.124e+01	8.684e+00	5.34e+00
Dim=30	*SDFV*	6.364e-01	4.594e+00	1.358e+01	3.576e-01
Dim=100	*C*	82%	65%	68%	76%
Function F2	MFV	5.609e+01	7.52e+02	7.00e+02	6.456e+02
Dim=100	SDFV	1.078e+02	3.027e+03	2.65e+02	2.564e+02
	C	78%	68%	71%	76%
Function F3	*MFV*	-4.190e+04	-4.021e+04	-4.102e+04	-4.231e+04
Dim=100	*SDFV*	8.320e+02	3.43e+03	1.75e+03	9.457e+02
	C	80%	72%	72%	77%
Function F4	*MFV*	3.21e-03	6.481e-03	4.28e-03	4.348e-04
Dim=100	*SDFV*	7.463e-04	2.41e-03	8.39e-04	7.569e-04
	C	72%	63%	67%	72%

confidence will decrease with the reduction of the swarm particles and also increase with the addition of the swarm particles. In all examples, the PSO-CS is able to reach the global minimum within the specified precision. Additionally, compared with PSO and CS algorithms, the standard deviation of the results with the hybrid PSO-CS is lower.

The survival and migration of avifauna inspired the inventions of both PSO and CS algorithms. The individual and social attributes are both considered in PSO, represented by *Pbest* and *Gbest*. The competition mechanism and a special flight pattern are constructed in CS. To improve the searching ability of traditional PSO algorithm, the utilization of CS algorithm's superiority is a conceivable way. The combination of these two algorithms is reasonable from the viewpoints of theory and realization. We apply this hybrid optimization algorithm to the engineering problems in the following part.

4. Engineering Applications I: Nonlinear Parameter Identification

Most systems encountered in the real world are nonlinear to some extent, and in many practical applications nonlinear models are required to achieve acceptable prediction accuracy. Modeling nonlinear systems therefore is of significant importance to the scientific community [18]. Parameter identification is an integrated part of modeling any products in engineering and industry. Nonlinear modeling problems are complex, and sometimes the mathematical model is not unique. In order to examine the PSO-CS algorithm's performance, it is now used to deal with the nonlinear parameter identification of the radar antenna servo system [8].

4.1. Formulation of the Nonlinear Parameter Identification Problem. Electromechanical turntable servo systems play important roles as the foundation and driving mechanisms of radars and telescopes. The nonlinearities, such as friction, backlash, and dead-zone, degrade the system performance, especially during rotation changes direction or some other conditions varying. Experiments are carried out in the servo turntable for missile-borne radar as shown in Figures 1 and 2. It is a single-input-single-output (SISO) system, in which the input variable is the voltage of the motor torque and the output variable is the elevation angle velocity.

We choose the chirp signal as the experimental test stimulation, with the frequency changing from 1 Hz to 10

Hz. Meanwhile, for cross-validation, another set of chirp and multitone signals are also used. Sampling time in this experiment is 10ms. The input filed data $u(k)$ and output data $y(k)$ are recorded and shown in Figure 3. It can be seen that the output elevation angle velocity signal distorts around the zero-crossing point. Because of the friction and other nonlinear characteristics, the curve of output signal has a flat roof in the middle around the zero-crossing point.

A nonlinear Hammerstein model is introduced to describe the input-output relationship with nonlinear characteristics for the turntable servo system. There is a nonlinear subsystem followed by the linear part with Hammerstein model as shown in Figure 4.

The structures and orders of the subsystems have been determined in former research [14, 15], $f(u(k)) = f_1u(k) + f_2u^2(k) + f_3u^3(k)$, $A(z) = 1 + a_1z^{-1} + a_2z^{-2} + a_3z^{-3}$, and $B(z) = b_0 + b_1z^{-1}$. Thus the nonlinear model of the radar turntable servo system can be expressed as $f(u(k)) = f_1u(k)+ f_2u^2(k) + f_3u^3(k)$ $A(z) = 1 + a_1z^{-1} + a_2z^{-2} + a_3z^{-3}$, and $B(z) = b_0 + b_1z^{-1}$. Thus the nonlinear model of the radar turntable servo system can be expressed as

$$\begin{aligned} x(k) &= f_1u(k) + f_2u^2(k) + f_3u^3(k) \\ &\left(1 + a_1z^{-1} + a_2z^{-2} + a_3z^{-3}\right) y(k) \\ &= z^{-1}\left(b_0 + b_1z^{-1}\right) x(k) \end{aligned} \tag{19}$$

The coefficients a_1, a_2, a_3, b_1, b_2, f_1, f_2, and f_3 need to be estimated. In the next step, the proposed PSO-CS algorithm is used to identify the Hammerstein nonlinear model of the radar antenna servo system. The fitness function should be able to describe the input-output relationship of the radar turntable servo system. The following equation is formulated, where the deviation between model output data and field experimental data is set as the fitness function and will be minimized.

$$Fitness\ function = \sum_{k=1}^{m} e^2(k) = \sum_{k=1}^{m} \left[y(k) - \hat{y}(k)\right]^2 \tag{20}$$

where $\hat{y}(k)$ is the estimated output of the model which is calculated iteratively in the PSO-CS algorithm and $y(k)$ is measured in the experiment as displayed in Figure 2. $e(k)$ is the error between field data $y(k)$ and model output $\hat{y}(k)$.

4.2. Application of PSO-CS Algorithm. Variable X in the proposed algorithm is set as $X = \{-\hat{a}_1, -\hat{a}_2, -\hat{a}_3, \hat{b}_1, \hat{b}_2, \hat{f}_1, \hat{f}_2, \hat{f}_3\}$, where symbol $\hat{}$ represents predicted/estimated/identified parameters in the simulation. Choose the parameters of the hybrid PSO-CS algorithm as in Table 7 for nonlinear identification simulation.

It is worth particularly pointing out that, in order to improve searching efficiency and narrow searching scope, the Recurrence Least Squares (RLS) method is introduced to data preprocess [18]. The effectiveness on this method is proved by our former research. Because of the mechanism constraints, the searching space (position and velocity) of the coefficients f_2 and f_3 is different from other coefficients in the Hammerstein model for the radar turntable servo system.

Figure 1: The employed instrument containing servo turntable for missile-borne radar.

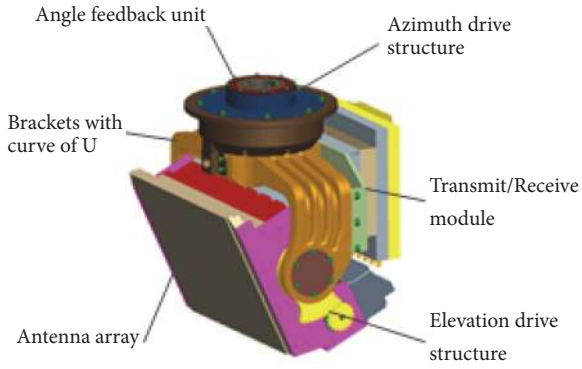

Figure 2: Three-dimension mechanical structure diagram of the servo for the missile-borne radar.

4.3. Results of PSO-CS and Comparison with Traditional Algorithms. The PSO-CS is performed several times with the final results listed in Table 8, and the calculation results of parameter estimation using PSO and CS are also shown. One of the convergence processes of the fitness function is shown in Figure 5.

In Table 4, the MFV and SDFV have the same definitions as those in Table 2. It is obvious that the mean and standard deviations of the fitness function with the hybrid PSO-CS algorithm are both less than the results from the PSO and CS.

4.4. Cross-Validation and Analysis. In order to estimate the fitness quality of the model through cross-validation with the consideration of curve fitting, the fitness quality $QF\%$ is defined as [7]

$$QF\% = \left(1 - \frac{(1/N)\sum_{n=1}^{N}\left(y(n) - y_{ident}(n)\right)^2}{(1/N)\sum_{n=1}^{N}\left(y(n)\right)^2}\right) \times 100\% \tag{21}$$

Table 7: Parameters in PSO-CS algorithm.

Meaning of parameter	Symbol	Value
Number of particles in the swarm	N	20
Dimension Length of vector variables representing the parameters to be identified	D	9
Maximum iteration	T	50
Number of data considered in error fitness function in Eq. (19)	m	5000
Acceleration coefficients	c_1, c_2	2
The friction of worst particles which are need to be replaced randomly	p_a	0.25
The index of exponential function in the Lèvy flight	β	3/2
Range of inertia weight factor	$[W_{\min}, W_{\max}]$	$[0.4, 0.9]$
Constrains of parameters a_1, a_2, a_3, b_1, b_2 and f_1	$[x_{\min 1}, x_{\max 1}]$ $[v_{\min 1}, v_{\max 1}]$	$[-3, 3]$ $[-0.3, 0.3]$
Constrains of parameter f_2, f_3	$[x_{\min 2}, x_{\max 2}]$ $[v_{\min 2}, v_{\max 2}]$	$[-0.3, 0.3]$ $[-0.03, 0.03]$

Table 8: Identified results of PSO-CS, PSO, and CS for Hammerstein model of radar turntable.

	a_1	a_2	a_3	b_0	b_1	f_1	f_2	f_3	*MFV*	*SDFV*
PSO-CS	-1.1294	-0.1675	0.0344	-1.2728	1.2737	-2.7388	-0.0896	-0.1	0.0301	0.0160
PSO	-1.1255	-0.1585	0.3485	-1.2401	1.2032	-2.6982	-0.086	-0.0966	0.1112	0.2295
CS	-1.2745	-0.1567	0.0345	-1.2728	1.2845	-2.7400	-0.0893	-0.99	0.0811	0.0473

The comparison between real and modeling output is shown in Figure 6. The fitness quality is $QF\% = 99.93\%$ for PSO-CS and only 91.71% and 92.33% for PSO and CS, respectively.

Figure 6 shows the comparison of the fitting curves of the three models with different coefficients and the measured result. It is no doubt that the performance of nonlinear Hammerstein model from PSO-CS algorithm is better than the ones from PSO or CS in the aspect of describing the input-output relationship of the radar turntable servo system.

From Table 2 and Figures 5 and 6, following conclusions can be drawn:

(a) Using the proposed PSO-CS algorithm, better values of fitness function are obtained in the searching process than the ones using PSO and CS.

(b) Figure 5 demonstrates that the result of PSO-CS algorithm is able to converge in less iteration.

(c) Three sets of parameters for Hammerstein models are obtained and listed in Table 4. Their performances are tested in several validation experiments as shown in Figure 6. From the fitting curves and QF% data, it is obvious that the model applied with PSO-CS is best among all.

The input and output characteristics of the Hammerstein models from the PSO-CS are in best agreement with the experimental data. Searching process with Lévy flights may take longer time than original optimization algorithm. Fortunately, the chance of local minima trapping is meanwhile minimized along with fast convergence which is verified in experiment. The novel algorithm outperforms the traditional PSO and CS optimization methods both in benchmark tests and in engineering application.

5. Engineering Application II: Optimal Reactive Power Dispatch (ORPD)

Management of reactive power resources is essential for secure and stable operation of power systems in the standpoint of voltage stability [3]. The ORPD problem is essential for the security and economic aspects of power system. As a subproblem of the optimal power flow calculation, it aims to minimize transmission losses or other concerned objective functions. In the past, computational intelligence-based techniques, such as seeker optimization algorithm [19], wo-point estimate method [20], teaching learning algorithm [21], PSO [22], differential evolution algorithm [23], oppositional krill herd algorithm [24], exchange market algorithm [25], and firefly algorithm [26] have been applied for solving ORPD problem. In [3], the PSO-imperialist competitive algorithm (PSO-ICA) is proposed and applied to the ORPD problem to minimize the total voltage deviation (TVD). In [27], a hybrid approach, based on the original differential evolution (DE) algorithm, combines variable scaling mutation and probabilistic state transition rule of the ant system to deal with the ORPD problem. In this part, the application of PSO-CS approach to the solution of ORPD problem is introduced in detail.

5.1. ORPD Problem Formulation

5.1.1. Objective Function. In most of the ORPD problem, the total loss minimization, voltage deviation reduction, and voltage stability improvement are concerned. In our research,

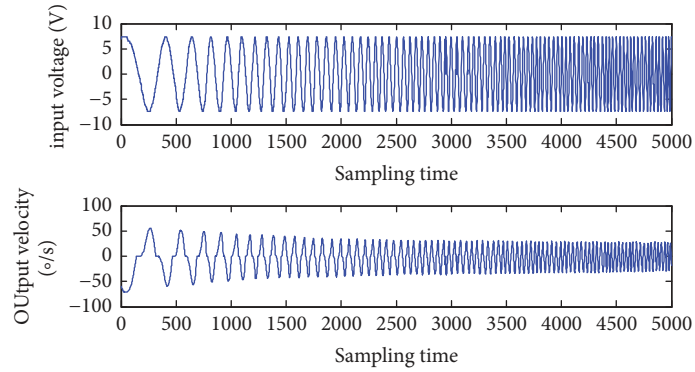

Figure 3: Input-output data for chirp signal of the servo turntable with 5000 sampling steps.

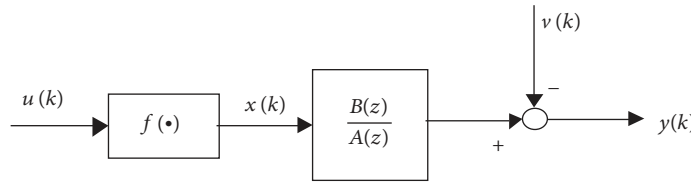

Figure 4: Structure of Hammerstein model.

the total loss minimization is the main function with the consideration of transformer tap setting and capacitor switching costs. It is defined as follows [28]:

$$F = \min\left[P_L + \lambda_1\left(\sum_{i=1}^{N_D}\frac{\Delta V_i}{V_{i\max} - V_{i\min}}\right)^2 + \lambda_2\left(\sum_{j=1}^{N_G}\frac{\Delta Q_j}{Q_{j\max} - Q_{j\min}}\right)^2 + C_T\Delta u_t + C_Q\Delta u_t\right] \quad (22)$$

where P_L is active power loss of the power system and V_i is the generator voltage of the i_{th} bus. $V_{i\max}$ and $V_{i\min}$ are the maximum and minimum generator voltages of the i_{th} bus, respectively. Q_j is the reactive power injection of the j_{th} transmission line. $Q_{j.\max}$ and $Q_{j.\min}$ are the maximum and minimum reactive power injections of the i_{th} transmission line, respectively. N_D is the total number of load nodes. N_G is the number of distributed generator. λ_1 and λ_2 are the cross-border penalty coefficients of load and reactive power generation, respectively. C_T and C_Q are the costs of transformer tap setting and capacitor switching, respectively. u_t contains the control variable at sampling time t, such as generator voltage, tap changing transformers, and number of shunt compensators [10, 18].

5.1.2. Inequality Constraints. In ORPD problem, the tap position of transformers, generator bus voltages, and the amount of the reactive power source installations are the independent variables. The limits of these variables are considered as inequality constraints.

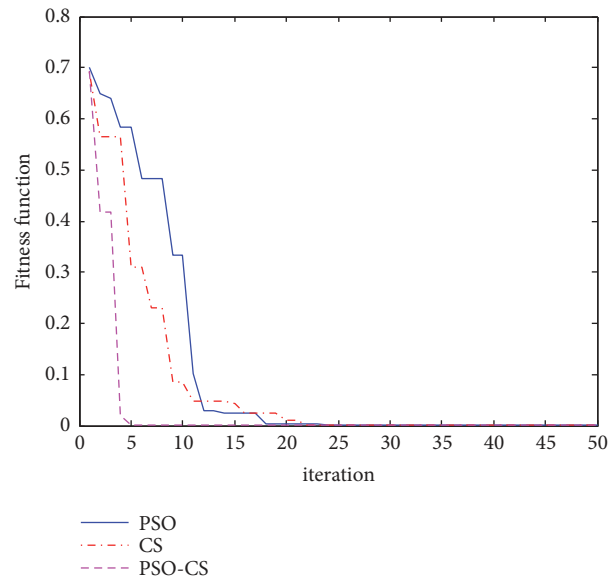

Figure 5: Convergence profiles for nonlinear parameter identification with PSO, CS, and hybrid PSO-CS.

$$\begin{aligned} V_{Gi.\min} \le V_{Gi} \le V_{Gi.\max} \quad & i = 1, 2, \ldots N_G \\ Q_{Cj.\min} \le Q_{Cj} \le Q_{Cj.\max} \quad & j = 1, 2, \ldots N_c \\ K_{Tk.\min} \le K_{Tk} \le K_{Tk.\max} \quad & k = 1, 2, \ldots N_t \end{aligned} \quad (23)$$

where $V_{Gi.\min}$ and $V_{Gi.\max}$ are the minimum and maximum generator voltages of the i_{th} bus, $Q_{Cj.\min}$ and $Q_{Cj.\max}$ are the minimum and maximum reactive power injections of the j_{th}

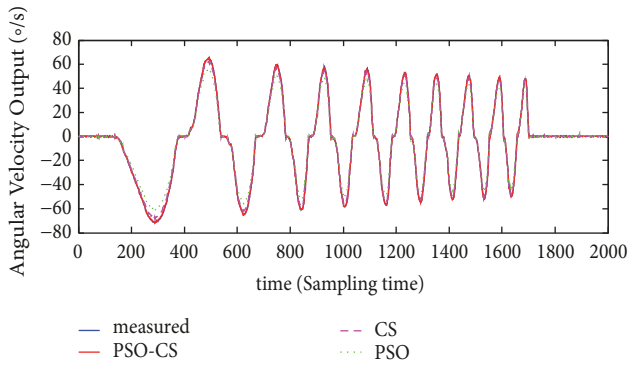

Figure 6: Comparison of the three models with PSO-CS, PSO, CS algorithm, and the measured field data.

Table 9: ORPD Results of PSO-CS, PSO, PSO-ICA and CS for IEEE 14-Bus system.

Variables	PSO-CS	PSO	PSO-ICA	CS
V_{G1}	1.040	0.950	1.100	0.965
V_{G2}	1.049	1.047	1.050	1.049
V_{G3}	1.007	1.008	1.007	1.0019
V_{G6}	1.059	1.052	1.037	0.958
V_{G8}	1.010	1.057	1.100	1.097
$T_{5,6}$	1.025	1.026	1.025	1.025
$T_{4,7}$	0.950	0.900	1.075	1.102
$T_{4,9}$	1.050	1.100	1.000	0.805
Q_9	0.100	1.100	0.975	0.900
Total loss	0.1862	0.1947	0.1864	0.1876

shunt compensator, $K_{Tk.\min}$ and $K_{Tk.\max}$ are the minimum and maximum tap setting of the k_{th} transmission line, N_c is the number of shunt compensators, and N_t is the number of tap changing transformers. The reactive power output of generators and load voltages are the dependent variables. Their limits are also modeled as

$$\begin{aligned} Q_{Gi.\min} \le Q_{Gi} \le Q_{Gi.\max} \quad & i = 1, 2, \ldots N_G \\ V_{Dj.\min} \le V_{Dj} \le V_{Dj.\max} \quad & j = 1, 2, \ldots N_D \end{aligned} \tag{24}$$

where $Q_{Gi.\min}$ and $Q_{Gi.\max}$ are the minimum and maximum reactive power generation of the i_{th} generator bus, respectively. $V_{Dj.\min}$ and $V_{Dj.\max}$ are the minimum and maximum voltage of the j_{th} load bus.

Besides, there are load bus voltage and the reactive power generation constraints as below.

$$\Delta V_i = \begin{cases} V_i - V_{i\max} & V_i > V_{i\max} \\ 0 & V_{i\min} \le V_i \le V_{i\max} \\ V_{i\max} - V_i & V_i < V_{i\min} \end{cases} \tag{25}$$

$$\Delta Q_j = \begin{cases} Q_j - Q_{j\max} & Q_j > Q_{j\max} \\ 0 & Q_{j\min} \le Q_j \le Q_{j\max} \\ Q_{j\min} - Q_j & Q_j < Q_{j\min} \end{cases} \tag{26}$$

5.1.3. Equality Constraint. The equality constraints of ORPD problem can be expressed as follows:

$$\begin{aligned} P_{Gi} - P_{Di} &= V_i \sum_{j \in i} V_j \left(G_{ij} \cos\theta_{ij} + B_{ij} \sin\theta_{ij} \right) \\ Q_{Gi} + Q_{Ci} - Q_{Di} &= V_i \sum_{j \in i} V_j \left(G_{ij} \sin\theta_{ij} - B_{ij} \cos\theta_{ij} \right) \end{aligned} \tag{27}$$

where P_{Gi} and Q_{Gi} are the active and reactive power generator of the i_{th} bus. P_{Di} and Q_{Di} are the active and reactive load demand of the i_{th} bus. G_{ij} and B_{ij} are the transfer conductance and susceptance between i_{th} and j_{th} bus, respectively. θ_{ij} is the voltage phase angle difference between i_{th} and j_{th} bus.

5.2. Proposed Methodology. The proposed hybrid PSO-CS is applied to the ORPD problem of IEEE 14-bus system. The researched IEEE14-bus system ($N_D = 14, N_G = 5$) consists of 5 generators and 3 transformers. The generators are located at buses 1, 2, 3, 6, and 8. The load tap transformers are set as $T_{5,6}$ $T_{4,7}$ $T_{4,9}$. The candidate reactive power compensation bus is node 9.

5.2.1. Individual Code and Constraints. The total loss of IEEE-14 bus system is calculated as Formula (21), and the constraints are defined as Formulas (23) to (27). The individual in PSO-CS application is encoded with the variables of generator voltages, reactive power compensator, and transmission tapes. Thus it is expressed as $x = [V_{G1}\ V_{G2}\ V_{G3}\ V_{G6}\ V_{G8}\ T_{5,6}\ T_{4,7}\ T_{4,9}\ Q_9]$.

The generator voltage V_{Gi} is set within the region of $[0.95, 1.1]$. Set B_k as the integer within $[-4, 4]$, and the transformer tap setting in our problem can be expressed as $T_k = 1 + B_k \times a_k$. Shut capacitor Q_i is defined as $Q_i = D_i \times a_i \times b_i$, in which b_i equals -1 in capacitive compensation and 1 in inductive compensation. The introductions of B_k and b_i form the ORPD into a mixed-integer problem.

Parameter Selection. The cross-border penalty coefficients of load and reactive power generation λ_1 and λ_2 are both selected as 500. The costs of transformer tap setting and capacitor switching, C_T and C_Q, are 7kw and 4kw per time, up to 10 times a day. Some parameters in PSO-CS are set as $N = 100$, $c_1 = c_2 = 2$, $W_{\max} = 0.9$, $W_{\min} = 0.4$, $\beta = 3/2$, and $p_a = 0.25$.

The power flow calculation in the ORPD problem is dealt with the Revised Newton Raphson method [8]. The pseudocode of the hybrid PSO-CS algorithm is shown as follows. The variables in the ORPD problem $X = \{x_1, \ldots, x_D\}$, $x_i = [V_{G1,i}\ V_{G2,i}\ V_{G3,i}\ V_{G6,i}\ V_{G8,i}\ T_{5,6,i}\ T_{4,7,i}\ T_{4,9,i}\ Q_{9,i}]$.

5.3. Results of ORPD Problem and Comparison. The ORPD program with the application of the hybrid PSO-CS algorithm is run 200 times. For comparison, the optimal solutions from the proposed method, traditional PSO, CS and hybrid PSO-ICA algorithms are all listed in Table 9. The fitness function of total loss reduces to 0.1862 using the hybrid PSO-CS

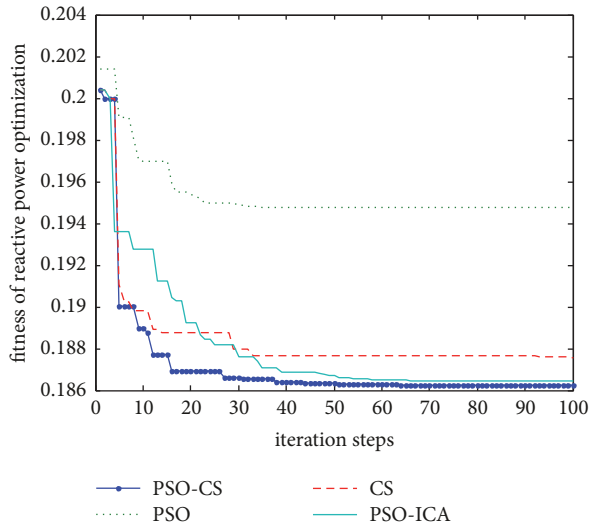

Figure 7: Comparison of the fitness functions for the IEEE 14-bus case using the PSO-CS, PSO, CS, and PSO-ICA.

algorithm. In the traditional PSO, original CS, and the hybrid PSO-ICA, the values are 0.1947, 0.1876, and 0.1864, which are higher than our proposed method. Convergence profiles of fitness function in ORPD for PSO-CS, PSO, CS, and PSO-ICA are demonstrated in Figure 7. It is demonstrated that the convergence profile of the proposed hybrid PSO-CS approach is also the promising one.

From this table, we can see that the PSO-CS technique is such an excellent hybrid global random search technique for ORPD problem and is structured incorporating the advantages of Cuckoo Search algorithm into particle swarm optimization (PSO). The quality of the proposed PSO-CS in application of ORPD has been compared with other prominent optimal methods such as PSO, CS, and PSO-ICA.

6. Conclusion

The hybrid PSO-CS algorithm has been proposed in this work. The approach is based on the combination of the basic PSO and CS algorithm. The selection scheme of individual and global best of PSO and the elimination mechanism and Lévy flight of CS constitute the key points in the new algorithm. The principal advantages are the high reliability and efficiency of the algorithm.

In the benchmark function test, the hybrid algorithm is able to find the global optimum. Besides, its standard deviation (SDFV) is low, indicating that the PSO-CS algorithm has good reliability and stability in finding an optimal solution. After the benchmark function test, the algorithm is applied to two different engineering problems.

In the first application, the hybrid PSO-CS algorithm is used to the parameter identification for the motor drive radar turntable servo system. Simulation results show that the PSO-CS algorithm further improves the identification accuracy of the Hammerstein model for the radar turntable and is more effective compared with traditional optimization algorithms. Then, the proposed hybrid approach is applied to the ORPD problem. The simulation result of the IEEE 14-bus system shows that the PSO-CS algorithm is capable of handling nonlinearity, multiple constraints, and multiple local minimum points in the ORPD problem.

Thus, the novel hybrid algorithm presents great superiority in obtaining the near-global optimum and effectiveness in solving nonlinear complicated engineering problems. The PSO-CS approach can be considered as a promising candidate for the future research and application.

Data Availability

The data used to support the findings of this study are available from the corresponding author upon request.

Conflicts of Interest

The authors declare that they have no conflicts of interest.

Acknowledgments

This study was supported by the National Key R&D Program of China (2016YFB0900400), Research Project of State Grid Corporation of China Anhui Province (5212001700), National Natural Science Foundations of China under Grant (51507001), and Doctoral Research Foundation of Anhui University under Grant (J01001929).

References

[1] Z. Bingül and O. Karahan, "A Fuzzy Logic Controller tuned with PSO for 2 DOF robot trajectory control," *Expert Systems with Applications*, vol. 38, no. 1, pp. 1017–1031, 2011.

[2] A. Gotmare, R. Patidar, and N. V. George, "Nonlinear system identification using a cuckoo search optimized adaptive Hammerstein model," *Expert Systems with Applications*, vol. 42, no. 5, pp. 2538–2546, 2015.

[3] M. Mehdinejad, B. Mohammadi-Ivatloo, R. Dadashzadeh-Bonab, and K. Zare, "Solution of optimal reactive power dispatch of power systems using hybrid particle swarm optimization and imperialist competitive algorithms," *International Journal of Electrical Power & Energy Systems*, vol. 83, pp. 104–116, 2016.

[4] D. H. Kim, "GA-PSO based vector control of indirect three phase induction motor," *Applied Soft Computing*, vol. 7, no. 2, pp. 601–611, 2007.

[5] E. Assareh, M. A. Behrang, M. R. Assari, and A. Ghanbarzadeh, "Application of PSO (particle swarm optimization) and GA (genetic algorithm) techniques on demand estimation of oil in Iran," *Energy*, vol. 35, no. 12, pp. 5223–5229, 2010.

[6] X. S. Yang and S. Deb, "Multi-objective cuckoo search for design optimization," *Computers & Operations Research*, vol. 40, pp. 1616–1624, 2013.

[7] O. Begambre and J. E. Laier, "A hybrid particle swarm optimization—simplex algorithm (PSOS) for structural damage identification," *Advances in Engineering Software*, vol. 40, no. 9, pp. 883–891, 2009.

[8] J. García, F. Altimiras, A. Peña et al., "A binary cuckoo search big data algorithm applied to large-scale crew scheduling

problems," *Complexity*, vol. 2018, Article ID 8395193, 15 pages, 2018.

[9] H. Chiroma, T. Herawan, I. Fister et al., "Bio-inspired computation: recent development on the modifications of the cuckoo search algorithm," *Applied Soft Computing*, vol. 61, pp. 149–173, 2017.

[10] Q. Zhang, Q. Wang, and G. Li, "Switched system identification based on the constrained multi-objective optimization problem with application to the servo turntable," *International Journal of Control, Automation, and Systems*, vol. 14, no. 5, pp. 1153–1159, 2016.

[11] Q. Zhang, Q. Wang, and G. Li, "Nonlinear modeling and predictive functional control of hammerstein system with application to the turntable servo system," *Mechanical Systems and Signal Processing*, vol. 72-73, pp. 383–394, 2016.

[12] R. B. Payne, M. D. Sorenson, and K. Klitz, *The Cuckoos*, Oxford University Press, NY, 2015.

[13] X. S. Yang, *Nature-Inspired Metaheuristic Algorithms*, Luniver Press, UK, 2nd edition, 2010.

[14] A. Ouaarab, B. Ahiod, and X.-S. Yang, "Discrete cuckoo search algorithm for job shop scheduling problem," in *Proceedings of the International Symposium on Intelligent Control (ISIC)*, pp. 1872–1876, IEEE, France, 2014.

[15] F. Zhao, Y. Liu, C. Zhang et al., "A self-adaptive harmony PSO search algorithm and its performance analysis," *Expert Systems with Applications*, vol. 42, no. 21, pp. 7436–7455, 2015.

[16] A. Alfi, "PSO with adaptive mutation and inertia weight and its application in parameter estimation of dynamic systems," *Acta Automatica Sinica*, vol. 37, no. 5, pp. 541–549, 2011.

[17] X. Li and M. Yin, "Modified cuckoo search algorithm with self adaptive parameter method," *Information Sciences*, vol. 298, pp. 80–97, 2015.

[18] R. Alireza and S. Scott, "Identification of nonlinear systems using NARMAX model," *Nonlinear Analysis Theory*, vol. 71, pp. 1198–1202, 2009.

[19] C. Dai, W. Chen, Y. Zhu, and X. Zhang, "Seeker optimization algorithm for optimal reactive power dispatch," *IEEE Transactions on Power Systems*, vol. 24, no. 3, pp. 1218–1231, 2009.

[20] S. M. Mohseni-Bonab, A. Rabiee, B. Mohammadi-Ivatloo et al., "A two-point estimate method for uncertainty modeling in multi-objective optimal reactive power dispatch problem," *International Journal of Electrical Power & Energy Systems*, vol. 75, pp. 194–204, 2016.

[21] B. Mandal and P. K. Roy, "Optimal reactive power dispatch using quasi-oppositional teaching learning based optimization," *International Journal of Electrical Power & Energy Systems*, vol. 53, no. 1, pp. 123–134, 2013.

[22] B. B. Pal, P. Biswas, and A. Mukhopadhyay, "GA based FGP approach for optimal reactive power dispatch," *Procedia Technology*, vol. 10, pp. 464–473, 2013.

[23] A. A. Abou El Ela, M. A. Abido, and S. R. Spea, "Differential evolution algorithm for optimal reactive power dispatch," *Electric Power Systems Research*, vol. 81, no. 2, pp. 458–464, 2011.

[24] S. Dutta, P. Mukhopadhyay, P. K. Roy et al., "Unified power flow controller based reactive power dispatch using oppositional krill herd algorithm," *International Journal of Electrical Power & Energy Systems*, vol. 80, pp. 10–25, 2016.

[25] A. Rajan and T. Malakar, "Exchange market algorithm based optimum reactive power dispatch," *Applied Soft Computing*, vol. 43, pp. 320–336, 2016.

[26] R. Liang, J. Wang, Y. Chen et al., "An enhanced firefly algorithm to multi-objective optimal active/reactive power dispatch with uncertainties consideration," *International Journal of Electrical Power & Energy Systems*, vol. 64, pp. 1088–1097, 2015.

[27] C.-M. Huang and Y.-C. Huang, "Combined differential evolution algorithm and ant system for optimal reactive power dispatch," *Energy Procedia*, vol. 14, pp. 1238–1243, 2012.

[28] J. Ding, Q. Zhang, and Y. Ma, "Optimal reactive power dispatch based on the CS-PSO algorithm," in *Proceedings of the 13th Conference on Industrial Electronics and Applications (ICIEA)*, IEEE, Wuhan, China, 2018.